QUARTERLY OF APPLIED MATHEMATICS
VOLUME XLVII, NUMBER 4
DECEMBER 1989, PAGES 691–704

LINEAR STABILITY ANALYSIS OF CYLINDRICAL FLAMES*

BY

MARC GARBEY, HANS G. KAPER, GARY K. LEAF, AND BERNARD J. MATKOWSKY

Argonne National Laboratory, Argonne, Illinois

Abstract. This article is concerned with the linear stability of cylindrical flames in a velocity field generated by a line source of fuel of constant strength $2\pi\kappa$ per unit length. The mathematical model involves the equations of mass and heat transfer in the regions on either side of the flame sheet and a set of jump conditions across the flame sheet. It admits a basic solution representing a stationary flame front in the shape of a circular cylinder at a radial distance κ from the line source. The circular front loses stability if either (i) the Lewis number of the reaction-limiting component is less than some critical value less than 1 and κ is greater than a critical value, or (ii) the Lewis number is greater than a critical value greater than 1. In the former case the circular front evolves into a steady cellular front, in the latter into a pulsating front, which may also be cellular. The WKB method is employed to derive approximations for the pulsating and cellular branches of the neutral stability curve.

1. Introduction. Experiments with laminar flames in gaseous combustible mixtures show that for certain mixtures a stationary smooth flame front may lose stability and break up into cells or evolve into a pulsating flame front with or without spatial structure; see, for example, [1], [2], [3], and [4]. This process is thought to be the first stage in the transition from laminar to turbulent flame propagation. Among the parameters that determine whether the process will occur and how it will evolve is the Lewis number, which measures the ratio of the thermal conductivity of the combustible mixture to the diffusivity of the reaction limiting component in the mixture. Cellular flames appear when the Lewis number is less than a critical value, which is less than 1; pulsating flames appear when the Lewis number is greater than a critical value, which is greater than 1.

The linear stability of a uniformly propagating plane flame front was studied by Sivashinsky [5]. Subsequently, Matkowsky, Putnick, and Sivashinsky [6] presented a

*Received December 5, 1988.

This work was supported by the Applied Mathematical Sciences subprogram of the Office of Energy Research, U. S. Department of Energy, under contract W-31-109-Eng-38 (M.G., H.G.K., G.K.L., B.J.M.) and grant DE-FG-0287-ER-25027 (M.G., B.J.M.).

Mailing address: Mathematics and Computer Science Division, Argonne National Laboratory, Argonne, IL 60439-4801.

Permanent address for Bernard J. Matkowsky: Department of Engineering Sciences and Applied Mathematics, Northwestern University, Evanston, IL 60208.

nonlinear theory describing the evolution of stationary cellular flames from perturbations of a cylindrical flame front. In the present article we pursue a linear theory that describes the onset of pulsating as well as stationary cellular flames. We derive approximations for the pulsating and celluar branches of the neutral stability curve, which separates the region where a stationary cylindrical flame is stable from the regions where it is unstable. The results of this theory provide critical information for a nonlinear computational study of cylindrical flames, which is currently in progress.

The model employed here is the same as in [6]. It was derived in [7] as an appropriate limit of the general equations governing flame propagation. The general equations are the nonlinear equations for conservation of mass and energy with first-order one-stage irreversible Arrhenius kinetics, and the equations of motion for the underlying gas flow of the combustible mixture. The limit assumed large activation energies, weak thermal expansion, and nearly comparable coefficients of heat and mass diffusion. In the limit, the fluid dynamics are decoupled from the chemistry and the transport processes, and the velocity field obtained from the fluid dynamic equations is a known coefficient in the equations of heat and mass transfer. The reaction zone is reduced to a moving free surface, termed the *flame front*, on which there is a heat source whose strength depends on the enthalpy perturbation at the front.

In this investigation we assume that the underlying flow field is generated by a line source of constant strength $2\pi\kappa$ per unit length. The resulting problem is therefore two-dimensional. The dependent variables measure the reduced temperature and enthalpy perturbation of the fuel mixture. The Lewis number L enters as a parameter into the problem. As stated above, the derivation of the model implies that L is close to 1; in fact, the difference $L - 1$ is $O(M^{-1})$, where M is the large parameter used in the large-activation-energy asymptotics. (More precisely, $M = N(1 - \sigma)$, where N is the nondimensional activation energy of the chemical reaction and $1 - \sigma$ is the relative temperature increase from the fresh mixture far upstream to the region behind the flame; $1 - \sigma$ is a measure of the thermal expansion of the gas in which the combustion process takes place.) We put

$$L = 1 + \frac{\lambda}{M}, \tag{1}$$

and use λ as a parameter in our investigations. The mathematical model is given in Sec. 2.

The model admits a nontrivial solution representing a stationary flame front in the shape of a circular cylinder at a radial distance κ from the line source. This solution, which we refer to as the basic solution, is introduced in Sec. 3. In the same section, we present the linear equations and the associated continuity, jump, and boundary conditions that govern the evolution of infinitesimal perturbations of the basic solution.

In Sec. 4, we show that the basic solution is linearly stable as long as $-2 < \lambda < 0$. If $\lambda < -2$, there exists a critical vlue κ_c, such that the basic solution is linearly stable for any $\kappa < \kappa_c$. As κ passes through κ_c, the basic solution loses stability and a transition to a cellular flame front occurs. These results agree with those in [6].

Section 5 contains the new results. Here we analyze the linear stability of the basic solution for positive values of λ, assuming that κ is large. Using a WKB analysis, we derive approximations for the neutral stability curve and show that the cylindrical front evolves into a pulsating cellular flame when λ exceeds a critical value λ_c. We first treat the case where the angular wave number n is $O(1)$ as $\kappa \to \infty$ (Sec. 5.1). Then we treat the case where $n = O(\kappa)$ as $\kappa \to \infty$ (Sec. 5.2) and show that the approximation for the pulsating branch thus obtained contains the approximation obtained earlier for the case $n = O(1)$ as a limiting case (Sec. 5.3). In other words, the approximation obtained in Sec. 5.2 is uniformly valid over the entire range of the wave number n, at least up to and including terms of the order $O(\kappa^{-2})$ as $\kappa \to \infty$. In Sec. 5.4 we show that the approximation for the neutral stability curve reduces to the (exact) expression for the cellular branch as the pulsation frequency vanishes. In the final Sec. 5.5 we present the graphs of the neutral stability curve for $\kappa = 10$ and $\kappa = 20$. These graphs were computed from the uniform approximation established in Sec. 5.2.

2. Mathematical model. The mathematical model used in this investigation is the same as in [6]. The dependent variables U and V measure the reduced temperature and enthalpy perturbation, respectively. They are functions of the radial variable r, the angular variable θ, and time t; U and V are 2π-periodic in θ.

The velocity field of the underlying fluid flow is generated by a line source of constant strength $2\pi\kappa$ per unit length. Thus, the velocity field is radial; its magnitude is $u = \kappa/r$.

The flame front is a surface of discontinuity for the derivatives of U and V. Its position is assumed to be of the form $r = F(\theta, t)$, where the function F is to be determined. The fresh mixture occupies the region $0 < r < F(\theta, t)$, the reaction products the region $r > F(\theta, t)$.

The governing equations are

$$U_t + \frac{\kappa}{r} U_r = \Delta U, \qquad V_t + \frac{\kappa}{r} V_r = \Delta V + \lambda \Delta U, \tag{2}$$

where Δ is the Laplacian in cylindrical coordinates, $\Delta = (1/r)(\partial/\partial r) r(\partial/\partial r) + (1/r^2)(\partial^2/\partial\theta^2)$.

The equations (2) are satisfied for $0 < r < F(\theta, t)$ and for $r > F(\theta, t)$. At the flame front ($r = F(\theta, t)$), U and V are continuous, but their gradients have jump discontinuities. Using the notation $[\cdot]$ to denote the difference between the limiting values as $r \to F(\theta, t)$ from above and below, we have

$$[U] = 0, \qquad [V] = 0, \tag{3}$$

$$[\mathbf{n} \cdot \operatorname{grad} U] + e^{V/2}|_{r=F(\theta,t)} = 0, \qquad [\mathbf{n} \cdot \operatorname{grad} V] - \lambda e^{V/2}|_{r=F(\theta,t)} = 0. \tag{4}$$

Here $\mathbf{n}$ is the unit vector normal to the front in the direction of increasing r,

$$\mathbf{n} = \frac{\operatorname{grad}(r - F(\theta, t))}{|\operatorname{grad}(r - F(\theta, t))|}\bigg|_{r=F(\theta,t)} = \frac{\{1, -F_\theta/F\}}{(1 + (F_\theta/F)^2)^{1/2}}.$$

Since $\operatorname{grad} U = \{U_r, (1/r)U_\theta\}$, it follows that

$$[\mathbf{n} \cdot \operatorname{grad} U] = \frac{[U_r] - (F_\theta/F^2)[U_\theta]}{(1 + (F_\theta/F)^2)^{1/2}}.$$

A similar expression holds for $[\mathbf{n} \cdot \operatorname{grad} V]$. In addition, U and V satisfy the limiting conditions

$$U \to 0, \qquad V \to 0 \quad \text{as } r \to 0, \tag{5}$$

$$U = 1 \quad \text{for all } r > F(\theta, t), \qquad V \text{ bounded as } r \to \infty. \tag{6}$$

3. Basic solution and linearized equations. The system of nonlinear equations (2), (3), (4), (5), and (6) admits the solution

$$F = \kappa, \tag{7}$$

$$U = U(r) = \begin{cases} \left(\frac{r}{\kappa}\right)^{\kappa}, & 0 < r < \kappa, \\ 1, & r > \kappa; \end{cases} \tag{8}$$

$$V = V(r) = \begin{cases} -\lambda\kappa \left(\frac{r}{\kappa}\right)^{\kappa} \log\left(\frac{r}{\kappa}\right), & 0 < r < \kappa, \\ 0, & r > \kappa. \end{cases} \tag{9}$$

We refer to this solution as the *basic solution.* It represents a stationary flame front in the shape of a circular cylinder at a radial distance $r = \kappa$ from the line source. At the front we have $[U_r]_{r=\kappa} = -1$, $[V_r]_{r=\kappa} = \lambda$, $[U_{rr}]_{r=\kappa} = -(\kappa - 1)/\kappa$, and $[V_{rr}]_{r=\kappa} = \lambda(2\kappa - 1)/\kappa$.

Upon linearization of (2), (3), (4), (5), and (6) around the basic solution, we obtain the following system of equations:

$$u_t + \frac{\kappa}{r} u_r = \Delta u, \qquad v_t + \frac{\kappa}{r} v_r = \Delta v + \lambda \Delta u, \tag{10}$$

for $0 < r < \kappa$ and $r > \kappa$;

$$[u]_{r=\kappa} - f = 0, \qquad [v]_{r=\kappa} + \lambda f = 0, \tag{11}$$

$$[u_r]_{r=\kappa} + \frac{1}{2} v(\kappa) - \frac{\kappa - 1}{\kappa} f = 0, \qquad [v_r]_{r=\kappa} - \frac{1}{2}\lambda v(\kappa) + \lambda \frac{2\kappa - 1}{\kappa} f = 0; \tag{12}$$

and

$$u \to 0, \qquad v \to 0 \quad \text{as } r \to 0, \tag{13}$$

$$u = 0 \quad \text{for all } r > \kappa, \qquad v \text{ bounded as } r \to \infty. \tag{14}$$

Here, f, u, and v are the perturbations of F, U, and V, respectively, about the corresponding quantities in the basic solution; in (12), the quantity $v(\kappa)$ is an abbreviation for $\lim_{\varepsilon \downarrow 0} v(\kappa + \varepsilon, \theta, t)$.

The system of equations (10) through (14) will be the object of investigation in the following sections.

4. Cellular flames.

The linearized system of equations (10), (11), 12), (13), and (14) admits nontrivial stationary solutions that are 2π-periodic in θ if

$$\lambda = -\frac{\kappa^2 + 4n^2}{n^2\kappa^2}(2n^2 + \kappa + (\kappa^2 + 4n^2)^{1/2}), \qquad n = 1, 2, \ldots . \tag{15}$$

If we interpret n as a continuous variable, then (15) defines a branch of the neutral stability curve in the (n,λ)-plane for any fixed value of κ. Of course, n is an integer, so solutions are realized only at discrete points on the curve. The basic solution evolves into a steady cellular flame front as one crosses the neutral stability curve in the direction of decreasing λ. For this reason we refer to this branch of the neutral stability curve as the *cellular branch*; it is in the lower half of the (n,λ)-plane, where the Lewis number is less than 1.

The equation (15) can also be recovered from [6, Eqs. (2.4), (2.5), and (2.6)].

The cellular branch of the neutral stability curve has a vertical asymptote at $n = 0$. It ascends monotonically to a maximum at some point $(n_c(\kappa),\lambda_c(\kappa))$, where $\lambda_c(\kappa) < -2$ for all κ, and descends monotonically to negative infinity as n increases; $n_c(\kappa) \sim \kappa^{3/4}$ and $\lambda_c(\kappa) \sim -2(1 + 4\kappa^{-1/2})$ as $\kappa \to \infty$. Graphs of the cellular branch are included in the figures in Sec. 5.

It follows that the basic solution is stable to infinitesimal perturbations for $-2 < \lambda < 0$, for any value of the (positive) parameter κ. If $\lambda < -2$, then there exists a critical value κ_c such that the basic solution is stable to infinitesimal perturbations for any $\kappa < \kappa_c$, but as κ passes through κ_c, the basic solution loses stability and a transition to a cellular flame front occurs.

If κ tends to infinity while $n = m\kappa$, $m = O(1)$, we have the exact expression

$$\lambda = -2(1 + 4m^2)\left(1 + \frac{1}{2m^2}(1 + (1 + 4m^2)^{1/2})\frac{1}{\kappa}\right). \tag{16}$$

We will see in Sec. 5.4 that this expression can be recovered from the approximation for the pulsating branch of the neutral stability curve if the pulsation frequency vanishes.

5. Pulsating flames. Next, we look for nonstationary solutions of (10) through (14) that are 2π-periodic in θ. In particular, we look for periodically oscillating solutions, whose temporal behavior is described by a factor $\exp(i\omega t)$, where ω is a nonzero constant, which may be complex. Such solutions describe, among others, traveling and standing waves on the flame front.

With only the r-dependence left, we use a prime to indicate differentiation with respect to r. Thus, (10) reduces to

$$\frac{1}{r}(ru')' - \frac{\kappa}{r}u' - \left(i\omega + \frac{n^2}{r^2}\right)u = 0, \tag{17}$$

$$\frac{1}{r}(rv')' - \frac{\kappa}{r}v' - \left(i\omega + \frac{n^2}{r^2}\right)v = -\lambda\left(\frac{1}{r}(ru')' - \frac{n^2}{r^2}u\right), \tag{18}$$

for $0 < r < \kappa$ and $r > \kappa$. The conditions (11), (12), (13), and (14) remain unchanged.

We introduce new independent and dependent variables, in order to transform the equations into a form that is amenable to a WKB analysis [8]. Let x be defined in terms of r,

$$x = \frac{\omega^{1/2}}{\kappa}r, \tag{19}$$

and let y and z be the following functions of x :

$$y(x) = \left(\frac{x}{r^\kappa}\right)^{1/2} u(r), \qquad z(x) = \left(\frac{x}{r^\kappa}\right)^{1/2} v(r). \tag{20}$$

Then y and z satisfy the equations

$$y'' + \kappa^2 \left\{ -\left(i + \frac{1}{4x^2}\right) + \left(\frac{1}{4} - n^2\right) \frac{1}{\kappa^2 x^2} \right\} y = 0, \tag{21}$$

and

$$\begin{aligned} z'' + \kappa^2 &\left\{ -\left(i + \frac{1}{4x^2}\right) + \left(\frac{1}{4} - n^2\right) \frac{1}{\kappa^2 x^2} \right\} z \\ &= -\lambda \left\{ y'' + \frac{\kappa}{x} y' + \frac{\kappa^2}{x^2} \left(\frac{1}{4} - \frac{1}{2\kappa} + \frac{1}{\kappa^2} \left(\frac{1}{4} - n^2 \right) \right) y \right\}. \end{aligned} \tag{22}$$

Here, a prime denotes differentiation with respect to x. These equations are in such a form that we can apply a WKB analysis for large values of κ. We pursue this idea in two cases, depending on the order of magnitude of n.

5.1. Case 1: $n = O(1)$ as $\kappa \to \infty$. In this subsection we consider the case where $n = O(1)$ as $\kappa \to \infty$.

We first solve for y (i.e., u). Two linearly independent solutions of (21) are $y_+(\cdot, \kappa)$ and $y_-(\cdot, \kappa)$,

$$y_\pm(\cdot, \kappa) = \exp(\kappa \chi_\pm(\cdot, \kappa)), \tag{23}$$

where

$$\chi_\pm(\cdot, \kappa) \sim \pm \chi_0(\cdot) + \kappa^{-1} \chi_1(\cdot) \pm \kappa^{-2} \chi_2(\cdot) + \kappa^{-3} \chi_3(\cdot) \pm \cdots, \qquad \kappa \to \infty; \tag{24}$$

with

$$\chi_0(x) = \frac{1}{2} \left\{ (1 + 4ix^2)^{1/2} - \log \frac{1 + (1 + 4ix^2)^{1/2}}{2xi^{1/2}} \right\}, \tag{25}$$

$$\chi_1(x) = -\frac{1}{2} \log \frac{(1 + 4ix^2)^{1/2}}{2xi^{1/2}}, \tag{26}$$

$$\chi_2(x) = -n^2 \log \frac{1 + (1 + 4ix^2)^{1/2}}{2xi^{1/2}} + \frac{1}{4(1 + 4ix^2)^{1/2}} - \frac{5}{12(1 + 4ix^2)^{3/2}}, \tag{27}$$

$$\chi_3(x) = \frac{\frac{1}{4} - n^2}{1 + 4ix^2} - \frac{3}{2(1 + 4ix^2)^2} + \frac{5}{4(1 + 4ix^2)^3}. \tag{28}$$

The limiting conditions at infinity eliminate any contribution from y_-. The contribution from y_+ follows upon application of the conditions (11) and (13). Thus we find

$$u(r) = \begin{cases} -\left(\dfrac{r}{\kappa}\right)^{(\kappa-1)/2} \dfrac{y_+(x(r), \kappa)}{y_+(\omega^{1/2}, \kappa)} f, & 0 < r < \kappa, \\ 0, & r > \kappa. \end{cases} \tag{29}$$

The solution v is found by considering first the region $r > \kappa$, where the equation (22) is homogeneous and the contribution from y_+ is zero, and then the region $0 < r < \kappa$, where the solution is a linear combination of y_+ and a particular solution of the

inhomogeneous equation. For the particular solution, it suffices to consider only the first few terms in the asymptotic expansion for large values of κ. Thus we find

$$v(r) = \begin{cases} \left(\frac{r}{\kappa}\right)^{(\kappa-1)/2} \frac{y_+(x(r),\kappa)}{y_+(\omega^{1/2},\kappa)}\{v(\kappa) + \lambda f[1 + \kappa\{g(x(r),\kappa) - g(\omega^{1/2},\kappa)\}]\}, & 0 < r < \kappa, \\ \left(\frac{r}{\kappa}\right)^{(\kappa-1)/2} \frac{y_-(x(r),\kappa)}{y_-(\omega^{1/2},\kappa)} v(\kappa), & r > \kappa; \end{cases} \tag{30}$$

where $v(\kappa) = \lim_{\varepsilon\to 0} v(\kappa + \varepsilon)$ is given by

$$v(\kappa) \sim \left\{1 - (1 + 4i\omega)^{1/2} - \frac{1}{\kappa}\left(1 + \frac{1}{1 + 4i\omega}\right) + \frac{1}{\kappa^2}\left(\frac{2(\frac{1}{4} - n^2)}{(1 + 4i\omega)^{1/2}} - \frac{3}{(1 + 4i\omega)^{3/2}} + \frac{5}{2(1 + 4i\omega)^{5/2}}\right) + \cdots\right\} f. \tag{31}$$

The function g has an asymptotic expansion,

$$g(\cdot,\kappa) \sim g_0(\cdot) + \kappa^{-1} g_1(\cdot) + \kappa^{-2} g_2(\cdot) + \cdots, \qquad \kappa \to \infty. \tag{32}$$

At this point, the derivatives of the coefficients are known,

$$g_0'(x) = \frac{1}{2x}\left\{\frac{1}{2}(1 + 4ix^2)^{1/2} + 1 + \frac{1}{2(1 + 4ix^2)^{1/2}}\right\}, \tag{33}$$

$$g_1'(x) = \frac{2ix}{(1 + 4ix^2)^2}, \tag{34}$$

$$g_2'(x) = -n^2\left\{\frac{1}{x(1 + 4ix^2)^{1/2}} - \frac{2ix}{(1 + 4ix^2)^{3/2}}\right\} + \frac{ix}{2(1 + 4ix^2)^{3/2}} + \frac{4ix}{(1 + 4ix^2)^{5/2}} - \frac{25ix}{2(1 + 4ix^2)^{7/2}}. \tag{35}$$

These expressions can be integrated, but the integrals are not needed, as only the derivatives of the coefficients g_i, $i = 0, 1, 2$, enter into the expression for λ. Finally, by applying (12), we obtain an asymptotic form of the dispersion relation,

$$\lambda \sim 2\frac{\phi_0(\omega) + \kappa^{-1}\phi_1(\omega) + \kappa^{-2}\phi_2(\omega) + \cdots}{\psi_0(\omega) + \kappa^{-1}\psi_1(\omega) + \kappa^{-2}\psi_2(\omega) + \cdots}, \tag{36}$$

where

$$\phi_0(\omega) = (1 + 4i\omega)^{3/2} - 1 - 4i\omega,$$

$$\phi_1(\omega) = 2 + 4i\omega,$$

$$\phi_2(\omega) = (4n^2 - 1)(1 + 4i\omega)^{1/2} - 2n^2 + \frac{1}{2} + \frac{6}{(1 + 4i\omega)^{1/2}} - \frac{3}{1 + 4i\omega} - \frac{5}{(1 + 4i\omega)^{3/2}} + \frac{5}{2(1 + 4i\omega)^2},$$

and

$$\psi_0(\omega) = 1 + 2i\omega - (1 + 4i\omega)^{1/2},$$

$$\psi_1(\omega) = \frac{4i\omega}{(1 + 4i\omega)^{3/2}},$$

$$\psi_2(\omega) = -2n^2 + \frac{(4n^2 + 1)i\omega}{1 + 4i\omega} + \frac{8i\omega}{(1 + 4i\omega)^2} - \frac{25i\omega}{(1 + 4i\omega)^3}.$$

Notice that the wave number n enters only in the second-order coefficients.

The equation for the neutral stability curve is found by setting $\operatorname{Im}\omega = 0$. If $\operatorname{Re}\omega \neq 0$, the basic solution evolves into a periodically pulsating cellular flame front as one crosses the neutral stability curve in the direction of increasing λ. This part of the neutral stability curve is therefore referred to as the *pulsating branch*. Its equation is obtained by eliminating $\operatorname{Re}\omega$ from (36). (Recall that the expression in the right member of (36) is complex, so the real and imaginary parts yield two distinct equations.)

The elimination process can be carried out asymptotically. Taking ω to be real, we assume that it is given by an expansion of the form

$$\omega \sim \omega_0 + \omega_1\kappa^{-1} + \omega_2\kappa^{-2} + \cdots, \tag{37}$$

and expand the coefficients ϕ_i and ψ_i, $i = 0, 1, 2$, in powers of κ^{-1}. Then we look for a real λ that has an asymptotic expansion of the form

$$\lambda \sim \lambda_0(n) + \lambda_1(n)\kappa^{-1} + \lambda_2(n)\kappa^{-2} + \cdots. \tag{38}$$

To lowest order, we have the complex equation

$$\lambda_0\psi_0(\omega_0) = 2\phi_0(\omega_0). \tag{39}$$

Separating the real and imaginary parts, we eliminate ω_0 and solve for λ_0. Since n does not enter at this order, we find that λ_0 is independent of n,

$$\lambda_0(n) \equiv \lambda_0 = 4(1 + \sqrt{3}) = 10.9282\ldots. \tag{40}$$

Once λ_0 is known, we find the value of ω_0 by substitution, $\omega_0 = \frac{1}{4}(3 + 2\sqrt{3})^{1/2} = 0.635615\ldots$.

In the next order, we have the complex equation

$$\lambda_1\psi_0(\omega_0) + \lambda_0\psi_0'(\omega_0)\omega_1 + \lambda_0\psi_1(\omega_0) = 2[\phi_0'(\omega_0)\omega_1 + \phi_1(\omega_0)]. \tag{41}$$

Again, separating the real and imaginary parts, we eliminate ω_1 and solve for λ_1. Since n still does not enter at this order, we find that λ_1 is also independent of n,

$$\lambda_1(n) \equiv \lambda_1 = 13.2376\ldots. \tag{42}$$

The numerical value of ω_1 is found to be $\omega_1 = 0.764368\ldots$.

The next coefficient in (38) is found from the complex equation

$$\begin{aligned}&\lambda_2\psi_0(\omega_0) + \lambda_1\psi_0'(\omega_0)\omega_1 + \lambda_1\psi_1(\omega_0)\\ &+ \lambda_0\left[\frac{1}{2}\psi_0''(\omega_0)\omega_1^2 + \psi_0'(\omega_0)\omega_2 + \psi_1'(\omega_0)\omega_1 + \psi_2(\omega_0)\right]\\ &\quad = 2\left[\frac{1}{2}\phi_0''(\omega_0)\omega_1^2 + \phi_2'(\omega_0)\omega_2 + \phi_1'(\omega_0)\omega_1 + \phi_2(\omega_0)\right].\end{aligned} \tag{43}$$

Note that the wave number n enters at this order. We find

$$\lambda_2(n) = 30.1350\ldots - 8n^2. \tag{44}$$

Thus we see that the pulsating branch of the neutral stability curve is parabolic and curving downward near $n = 0$.

We observe that the expansion (38) breaks down when n is of the same order as κ, because of the term n^2 in the coefficient $\lambda_2(n)$. This observation leads us to consider the case where $n = O(\kappa)$ as $\kappa \to \infty$.

5.2. Case 2. $n = O(\kappa)$ as $\kappa \to \infty$. We consider the case where

$$n = m\kappa, \qquad m = O(1), \qquad \kappa \to \infty. \tag{45}$$

We use the abbreviations

$$4_m = \frac{4}{1+4m^2}, \qquad 2_m = \frac{2}{(1+4m^2)^{1/2}}. \tag{46}$$

The differential equations (21) and (22) assume the form

$$y'' + \kappa^2 \left\{ -\left(i + \frac{1}{4_m x^2} \right) + \frac{1}{4\kappa^2 x^2} \right\} y = 0, \tag{47}$$

and

$$\begin{aligned} z'' + \kappa^2 &\left\{ -\left(i + \frac{1}{4_m x^2} \right) + \frac{1}{4\kappa^2 x^2} \right\} z \\ &= -\lambda \left\{ y'' + \frac{\kappa}{x} y' + \frac{\kappa^2}{x^2} \left(\frac{1}{4} - m^2 - \frac{1}{2\kappa} + \frac{1}{4\kappa^2} \right) y \right\}. \end{aligned} \tag{48}$$

Again, a prime denotes differentiation with respect to x.

The approach is very similar to the one followed in the previous subsection. In fact, we shall use the same symbols to denote corresponding quantities. We first solve for y (i.e., u). Two linearly independent solutions of (21) are $y_+(\cdot, \kappa)$ and $y_-(\cdot, \kappa)$,

$$y_\pm(\cdot, \kappa) = \exp(\kappa \chi_\pm(\cdot, \kappa)), \tag{49}$$

where

$$\chi_\pm(\cdot, \kappa) \sim \pm\chi_0(\cdot) + \kappa^{-1}\chi_1(\cdot) \pm \kappa^{-2}\chi_2(\cdot) + \kappa^{-3}\chi_3(\cdot) \pm \cdots, \qquad \kappa \to \infty; \tag{50}$$

with

$$\chi_0(x) = \frac{2}{4_m} \left\{ (1 + 4_m i x^2)^{1/2} - \log \frac{1 + (1 + 4_m i x^2)^{1/2}}{2x i^{1/2}} \right\}, \tag{51}$$

$$\chi_1(x) = -\frac{1}{2} \log \frac{(1 + 4_m i x^2)^{1/2}}{2x i^{1/2}}, \tag{52}$$

$$\chi_2(x) = \frac{2_m}{8(1 + 4_m i x^2)^{1/2}} - \frac{5 \cdot 2_m}{24(1 + 4_m i x^2)^{3/2}}. \tag{53}$$

As in the previous subsection we find

$$u(r) = \begin{cases} -\left(\dfrac{r}{\kappa} \right)^{(\kappa-1)/2} \dfrac{y_+(x(r), \kappa)}{y_+(\omega^{1/2}, \kappa)} f, & 0 < r < \kappa, \\ 0, & r > \kappa; \end{cases} \tag{54}$$

and

$$v(r) = \begin{cases} \left(\frac{r}{\kappa}\right)^{(\kappa-1)/2} \frac{y_+(x(r),\kappa)}{y_+(\omega^{1/2},\kappa)}\{v(\kappa) + \lambda f[1 + \kappa\{g(x(r),\kappa) - g(\omega^{1/2},\kappa)\}]\}, & 0 < r < \kappa, \\ \left(\frac{r}{\kappa}\right)^{(\kappa-1)/2} \frac{y_-(x(r),\kappa)}{y_-(\omega^{1/2},\kappa)} v(\kappa), & r > \kappa; \end{cases} \tag{55}$$

where $v(\kappa) = \lim_{\varepsilon \to 0} v(\kappa + \varepsilon)$ is given by

$$v(\kappa) \sim \left\{1 - \frac{2}{2_m}(1 + 4_m i\omega)^{1/2} - \frac{1}{\kappa}\left(1 + \frac{1}{1 + 4_m i\omega}\right) + \frac{2_m}{2\kappa^2}\left(\frac{1}{2(1 + 4_m i\omega)^{1/2}} - \frac{3}{(1 + 4_m i\omega)^{3/2}} + \frac{5}{2(1 + 4_m i\omega)^{5/2}}\right) + \cdots\right\} f. \tag{56}$$

The function g has an asymptotic expansion,

$$g(\,\cdot\,,\kappa) \sim g_0(\cdot) + \kappa^{-1} g_1(\cdot) + \kappa^{-2} g_2(\cdot) + \cdots, \qquad \kappa \to \infty. \tag{57}$$

At this point, the derivatives of the coefficients are known,

$$g_0'(x) = \frac{1}{2x}\left\{\frac{1}{2_m}(1 + 4_m i x^2)^{1/2} + 1 + \frac{1}{2(1 + 4_m i x^2)^{1/2}}\right\}, \tag{58}$$

$$g_1'(x) = 4_m\left(\frac{1}{4} - m^2\right)\frac{2ix}{(1 + 4_m i x^2)^2}, \tag{59}$$

$$g_2'(x) = \frac{2_m}{16x}\left\{\frac{1}{(1 + 4_m i x^2)^{1/2}} - \frac{6}{(1 + 4_m i x^2)^{3/2}} + \frac{5}{(1 + 4_m i x^2)^{5/2}}\right\} + 4_m\left(\frac{1}{4} - m^2\right)\frac{2_m}{16x}\left\{\frac{13}{(1 + 4_m i x^2)^{3/2}} - \frac{38}{(1 + 4_m i x^2)^{5/2}} + \frac{25}{(1 + 4_m i x^2)^{7/2}}\right\}. \tag{60}$$

These expressions can be integrated, but, as before, the integrals are not needed. Application of the jump condition(12) results in the following asymptotic expression for the dispersion relation:

$$\lambda \sim 2\frac{\phi_0(\omega) + \kappa^{-1}\phi_1(\omega) + \kappa^{-2}\phi_2(\omega) + \cdots}{\psi_0(\omega) + \kappa^{-1}\psi_1(\omega) + \kappa^{-2}\psi_2(\omega) + \cdots}, \tag{61}$$

where

$$\phi_0(\omega) = \frac{4}{4_m}(1 + 4_m i\omega)^{3/2} - \frac{2}{2_m}(1 + 4_m i\omega),$$

$$\phi_1(\omega) = \frac{2}{2_m}(1 + 4_m i\omega) + \frac{2}{2_m},$$

$$\phi_2(\omega) = -(1 + 4i\omega)^{1/2} + \frac{2_m}{4} + \frac{6}{(1 + 4_m i\omega)^{1/2}} - \frac{3 \cdot 2_m}{2(1 + 4_m i\omega)} - \frac{5}{(1 + 4_m i\omega)^{3/2}} + \frac{5 \cdot 2_m}{4(1 + 4_m i\omega)^2},$$

and

$$\psi_0(\omega) = \frac{2_m}{2}(1 + 2i\omega) - (1 + 4_m i\omega)^{1/2},$$
$$\psi_1(\omega) = \frac{4_m}{4}(1 - 4m^2)\frac{4_m i\omega}{(1 + 4_m i\omega)^{3/2}},$$

$$\psi_2(\omega) = \frac{2_m}{8} + \frac{2_m(13 \cdot 4_m(1 - 4m^2) - 24)}{32(1 + 4_m i\omega)} - \frac{2_m(38 \cdot 4_m(1 - 4m^2) - 20)}{32(1 + 4_m i\omega)^2} + \frac{2_m \cdot 25 \cdot 4_m(1 - 4m^2)}{32(1 + 4_m i\omega)^3}.$$

Notice that the reduced wave number m is already present in the lowest-order coefficients.

The equation for the neutral stability curve is found from (61) by setting $\operatorname{Im}\omega = 0$ and eliminating $\operatorname{Re}\omega$, as in the previous subsection. However, this time the computations are considerably more involved, because of the fact that m enters already in the $O(1)$-terms. In fact, with λ of the form

$$\lambda \sim \lambda_0(m) + \lambda_1(m)\kappa^{-1}\lambda_2(m)\kappa^{-2} + \cdots, \tag{62}$$

we can find the leading term in the expansion,

$$\lambda_0(m) = 4\frac{1 + 8m^2}{1 + 12m^2}(1 + (3 + 24m^2)^{1/2}). \tag{63}$$

The higher-order terms can be computed numerically, using the same algorithm as in the previous subsection. Graphs of the pulsating branch of the neutral stability curve computed from (61) are included in the figures to be presented in Sec. 5.5.

5.3. Uniform expansion. We now compare the expressions (36) and (61) for the dispersion relation. In order to make the comparison, we set $m = n/\kappa$ in (61) and let κ tend to infinity, while keeping $n = O(1)$.

In the limit when $\kappa = \infty$, $4_m = 4$ and $2_m = 2$, so $\phi_0(\omega)$ in (61) coincides with $\phi_0(\omega)$ in (36), and the same is true for ψ_0. Thus, to leading order, the two expressions are identical. This conclusion is confirmed by the fact that the expression for the leading coefficient $\lambda_0(m)$ in the expansion (62) tends to the constant value $4(1 + \sqrt{3})$, which is precisely the value of the leading coefficient λ_0 in (38).

Next, by substituting an asymptotic expansion for ω in powers of κ^{-1}, with coefficients that depend on n, we can compare the coefficients ϕ_i and ψ_i, $i = 0, 1, 2$, in (61) and (36), at least to $O(\kappa^{-2})$. The computations are tedious, although straightforward, and confirm that the coefficients indeed agree. Hence, the expression (61) for the dispersion relation, and therefore the resulting expansion (62) for the pulsating branch of the neutral stability curve, are uniformly valid over the entire range of wave numbers, at least to $O(\kappa^{-2})$. In other words, (62) may be considered as a uniform expansion (within the limits of the current approximation) for the pulsating branch of the neutral stability curve.

5.4. Cellular flames—revisited. The expression for the pulsating branch of the neutral stability curve was found from (61) by requiring that $\operatorname{Im}\omega = 0$ and assuming that $\operatorname{Re}\omega \neq 0$. If, in addition, we require that $\operatorname{Re}\omega = 0$, so that in effect $\omega = 0$, we should recover the expression for the cellular branch of the neutral stability curve. This gives an additional check on the correctness of the formulae presented in this section.

The exact expression for the cellular branch is given in terms of m in (16),

$$\lambda = -2(1 + 4m^2)\left(1 + \frac{1}{2m^2}(1 + (1 + 4m^2)^{1/2})\frac{1}{\kappa}\right). \tag{64}$$

On the other hand, if we set $\omega = 0$ in (61), we obtain

$$\lambda = -2(1 + 4m^2)\left(1 - \frac{2}{1 - (1 + 4m^2)^{1/2}}\frac{1}{\kappa}\right). \tag{65}$$

The two expressions are identical, as they should be.

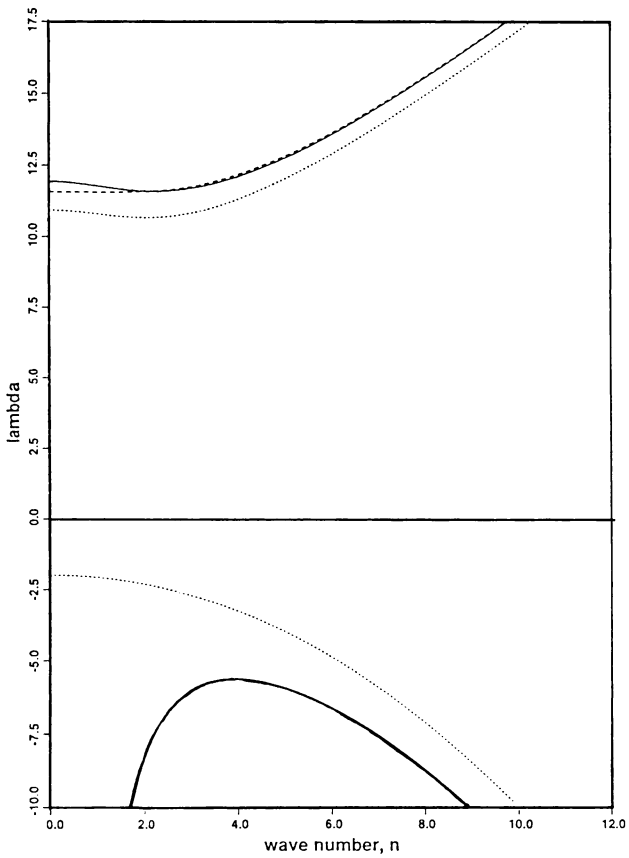

FIG. 1. Neutral stability curves for $\kappa = 10$. The dotted curves represent the leading term in the approximation ($\kappa = \infty$), the dashed curve includes the $O(\kappa^{-1})$-correction terms, and the solid curves include the $O(\kappa^{-2})$-correction terms.

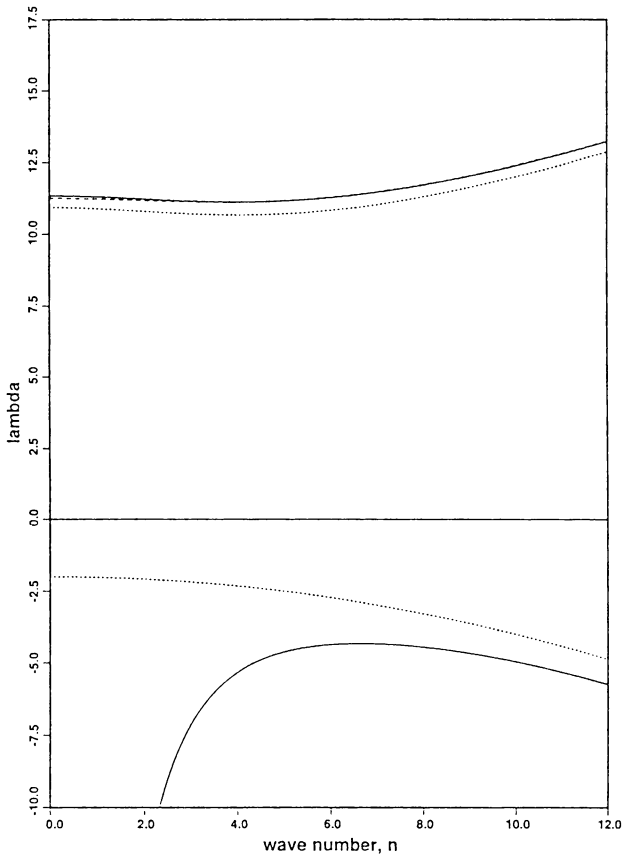

FIG. 2. Neutral stability curves for $\kappa = 20$. The dotted curves represent the leading term in the approximation ($\kappa = \infty$), the dashed curve includes the $O(\kappa^{-1})$-correction terms, and the solid curves include the $O(\kappa^{-2})$-correction terms.

5.5. Numerical results. We illustrate our results in two cases, $\kappa = 10$ and $\kappa = 20$. Figures 1 and 2 give the graphs of the neutral stability curve. The horizontal coordinate is the wave number n ($n = m\kappa$), the vertical coordinate is λ. The cellular branch is in the lower part, the pulsating branch in the upper part of each figure.

The cellular branches (solid curves) were computed from the exact formula (15), the pulsating branches from the uniform approximation (62). We also give the graphs in the limiting case $\kappa = \infty$ (dotted curves). Notice that in this limit the cellular branch intersects the vertical axis at $\lambda = -2$; when κ is finite, the vertical axis is an asymptote for the cellular branch. To illustrate the effect of finite κ, we computed both the $O(\kappa^{-1})$-approximation (dashed curves) and the $O(\kappa^{-2})$-approximation (solid curves) to the pulsating branches. Clearly, the approximation becomes better as κ increases.

REFERENCES

[1] F. A. Williams, *Combustion Theory*, 2nd ed., Benjamin/Cummings, Reading, Mass., 1985

[2] J. D. Buckmaster and G. S. S. Ludford, *Theory of Laminar Flames*, Cambridge University Press, Cambridge, 1982

[3] J. D. Buckmaster and G. S. S. Ludford, *Lectures on Mathematical Combustion*, CBMS–NSF Regional Conference Series in Applied Mathematics, Vol. 43, SIAM, Philadelphia, 1983

[4] G. H. Markstein, *Nonsteady Flame Propagation*, MacMillan, New York, 1964

[5] G. I. Sivashinsky, *Diffusional thermal theory of cellular flames*, Combustion Science and Technology **15**, 137–145 (1977)

[6] B. J. Matkowsky, L. J. Putnick, and G. I. Sivashinsky, *A nonlinear theory of cellular flames*, SIAM J. Appl. Math. **38**, 489–504 (1980)

[7] B. J. Matkowsky and G. I. Sivashinsky, *An asymptotic derivation of two models in flame theory associated with the constant density approximation*, SIAM J. Appl. Math. **37**, 686–700 (1979)

[8] J. Murray, *Asymptotic Analysis*, Springer-Verlag, New York, 1984